Critical properties in single crystals of $Pr_{1-x}Pb_xMnO_3$

B. Padmanabhan,[1,*] H. L. Bhat,[1] Suja Elizabeth,[1] Sahana Rößler,[2,3,4] U. K. Rößler,[2] K. Dörr,[2] and K. H. Müller[2]
[1]*Department of Physics, Indian Institute of Science, Bangalore 560012, India*
[2]*IFW Dresden, Postfach 270016, D-01171 Dresden, Germany*
[3]*Institut für Festkörperphysik, Technische Universität Dresden, D-01062 Dresden, Germany*
[4]*Max-Planck-Institut für Chemische Physik fester Stoffe, Nöthnitzer Strasse 40, D-01187 Dresden, Germany*
(Received 9 October 2006; revised manuscript received 12 December 2006; published 16 January 2007)

The critical properties at the ferromagnetic-paramagnetic transition have been analyzed from data of static magnetization measurements on single crystals of $Pr_{1-x}Pb_xMnO_3$ for $x=0.23$ and $x=0.30$. In $Pr_{1-x}Pb_xMnO_3$, the ferromagnetic ordering and the metal-insulator transition do not coincide in parts of the phase diagram. The crystal with $x=0.23$ is a ferromagnetic insulator with Curie temperature $T_C=167$ K, while the crystal with $x=0.30$ has $T_C=198$ K and remains metallic up to a metal-insulator transition temperature $T_{MI}=235$ K. The dc magnetization measurements were carried out in the field range from 0 to 5 T for an interval in the critical temperature range $T_C\pm10$ K corresponding to a reduced temperature interval $0.003<|\epsilon|<0.06$. The exponents β for spontaneous magnetization, γ for the initial susceptibility above T_C, and δ for the critical magnetization isotherm at T_C were obtained by static scaling analysis from modified Arrott plots and by the Kouvel-Fisher method for the insulating crystal with composition $x=0.23$. The data are well described by critical exponents similar to those expected for the Heisenberg universality class relevant for conventional isotropic magnets. Systematic deviations from scaling in the data for the metallic crystal with composition $x=0.30$ are demonstrated from effective critical exponents near the assumed ordering transition. The unconventional magnetic ordering in this system suggests the presence of frustrated magnetic couplings that suppress magnetic ordering and lower the transition temperature.

DOI: 10.1103/PhysRevB.75.024419 PACS number(s): 75.47.Gk, 64.60.Fr, 75.40.Cx, 71.27.+a

I. INTRODUCTION

The paramagnetic (PM)-ferromagnetic (FM) transition accompanied by the metal-insulator (MI) transition in metallic ferromagnetic manganites ($R_{1-x}A_xMnO_3$; R=La, Pr, etc., and A=Ca, Sr, etc.) is the result of a crossover from localization to delocalization of charge carriers.[1,2] Due to the strong coupling between the itinerant e_g electrons and Jahn-Teller phonons, the MI transition can be described as a discontinuous transition between the mobile and localized polarons. Hence, Archibald *et al.*[3] suggested that the accompanying FM-PM transition should also be of first order. Contrary to this, most of the manganites show a second-order phase transition at T_C. The usual perception that the FM-PM transitions are of second order is corroborated by the absence of hysteresis in the temperature variation of magnetization and the observation of a smaller entropy change from specific heat data across the transition.

Theoretical investigations on the critical behavior of colossal magnetoresistive (CMR) manganites by Motome and Furukawa[4] based on simplified DE models reveal that the FM-PM transition should belong to the Heisenberg universality class. The Heisenberg model assumes short-range interactions between localized spins, but the range of exchange interactions in CMR manganites is not obvious due to the itinerant nature of the e_g electrons and the close link between metallic conductivity and ferromagnetism. Therefore, it is not clear whether the ferromagnetic manganites should generically behave like conventional isotropic magnets with a FM-PM transition belonging to the Heisenberg universality class.

The magnetic properties of $Pr_{1-x}Pb_xMnO_3$ are less studied when compared to other rare-earth manganites. The physical properties of Pb-doped $PrMnO_3$ differ from those of the La-based manganites since Pr^{3+} has lower ionic radii than La and also a net magnetic moment due to unpaired f shell electron. Thus, $Pr_{1-x}Pb_xMnO_3$ has a reduced average radius of the A-site ions, $\langle r_A\rangle$, and hence a lower T_C. Interestingly, in a certain doping range, this manganite system shows a rather wide temperature difference between the MI transition temperature T_{MI} and the Curie temperature T_C with $T_{MI}>T_C$.[5] This is unusual because in the majority of the mixed-valent ferromagnetic manganites, one finds $T_C\simeq T_{MI}$.

Indeed, assuming that the DE mechanism is responsible for the ferromagnetic order, we find it difficult to explain a wide intermediate paramagnetic phase with metal-like conductivity. At lower doping, one finds a transition between an insulating paramagnetic phase into a ferromagnetic insulating phase. However, in the vicinity of T_C, a metal-like conductivity behavior is observed.[5]

In a simple picture, the presence of a band of mobile carriers should mediate a sufficiently strong ferromagnetic exchange to drive a ferromagnetic ordering transition. A few antiferromagnetic manganites with metallic conductivity are known, such as the $La_{1-x}Sr_xMnO_3$ near $x\sim0.6$ where itinerant charge transport takes place in an A-type antiferromagnetically ordered state with alternately stacked ferromagnetic planes.[6]

Also, the presence of PM-FM transitions in mixed-valent manganites without a metal-like conductivity is well known and mechanisms to explain such phases have been proposed.[7] Here, localization of carriers due to strong electron-lattice coupling via Jahn-Teller effects or disorder may prevent metallic conductivity, while the DE-exchange mechanism remains sufficiently strong to ensure a PM-FM

transition. In view of the unusual phase diagram of the $Pr_{1-x}Pb_xMnO_3$ system, an investigation on the critical point phenomena at its PM-FM transition and a comparison between the insulating and the metallic ferromagnets from this system are of high interest to disentangle the mechanisms leading to ferromagnetic order and to MI transitions in the mixed-valent manganites.

II. METHODS

A. Experimental details

Single crystals of $Pr_{1-x}Pb_xMnO_3$ were grown by the flux technique.[8] The phase was confirmed by powder x-ray diffraction, and compositions were determined by energy dispersive x-ray analysis and subsequently by inductively coupled plasma atomic emission spectroscopy for higher precision. From the grown crystals, two compositions, $x=0.23$ and $x=0.30$, were selected for the present study. Basic physical properties of the crystals from this compound series have been determined earlier, as reported in Ref. 5. The crystal with composition $x=0.23$ is a ferromagnetic insulator, while the crystal with $x=0.3$ undergoes a MI transition at 235 K with a peak magnetoresistance value of 93% near T_{MI}.[5] For the present studies, dc magnetization measurements M vs H were carried out in the temperature range from 155 to 179 K for $x=0.23$ and from 188 to 214.5 K for $x=0.30$ in external fields of up to 5 T to cover the magnetic transition. The magnetization measurements were carried out by using commercial superconducting quantum interference device magnetometer (Quantum Design). The magnetic field was applied along the long edge of the platelet-shaped crystals to minimize demagnetization effects. The orientation of these crystals has been determined by x-ray diffraction. It shows that the magnetic field has been oriented within a few degrees along a $\langle 100 \rangle$ direction of the pseudocubic perovskite crystal structure of our crystals. The effective internal field H_{eff} used for the scaling analysis has been corrected for demagnetization, $H_{\text{eff}}=H_{\text{appl}}-D_aM$, where D_a is the demagnetization factor obtained from M vs H measurements in the low-field linear-response regime at 10 K.

B. Scaling analysis

The critical properties of a magnetic system showing a second-order phase transition are characterized by critical exponents α, β, γ, and δ and the magnetic equation of state which connects the four exponents. The exponent α can be obtained from specific heat and β and γ from spontaneous magnetization and initial susceptibility, below and above T_C, respectively, while δ is the critical isotherm exponent. The mathematical definitions of the exponents from magnetization measurements are given below: Below T_C, the temperature dependence of the spontaneous magnetization $M_S(T)$ is given by

$$M_S(T) = M_0|\epsilon|^{-\beta}, \quad \epsilon < 0 \quad \text{for } H \to 0, \tag{1}$$

where $\epsilon=(T-T_C)/T_C$.

Above T_C, the initial susceptibility is given by

$$\chi_0^{-1}(T) = (h_0/M_0)\epsilon^{\gamma}, \quad \epsilon > 0. \tag{2}$$

At T_C, M and H are related by

$$M = DH^{1/\delta}, \quad \epsilon = 0. \tag{3}$$

Here, M_0, h_0/M_0, and D are the critical amplitudes.

In the critical region, the magnetic equation of state is given by

$$M(H,\epsilon) = |\epsilon|^{\beta} f_{\pm}(H/|\epsilon|^{\beta+\gamma}), \tag{4}$$

where f_+ for $T>T_C$ and f_- for $T<T_C$ are regular analytic functions. Equation (4) implies that $M/|\epsilon|^{\beta}$ as a function of $H/|\epsilon|^{\beta+\gamma}$ yields two universal curves, one for temperatures below T_C and the other for temperatures above T_C.

If a magnetic system is governed by various competing couplings and/or randomness, the properties in the critical region may show various systematic trends or crossover phenomena. In that case, it is useful to generalize the power laws for the critical behavior by defining effective exponents through

$$\beta_{\text{eff}} = -\frac{d(\ln M_S(\epsilon))}{d(\ln \epsilon)}, \quad \gamma_{\text{eff}} = -\frac{d(\ln \chi_0(\epsilon))}{d(\ln \epsilon)}, \tag{5}$$

which depend on the separation ϵ from the critical point.[9–11]

In the asymptotic limit $\epsilon \to 0$, the effective exponents approach the universal critical (asymptotic) exponent. The calculations of the logarithmic derivatives involve large uncertainties. Therefore, we have used two different methods to obtain estimates on effective exponents: (i) The complete set of data $\ln M(\epsilon)$ or $\ln \chi(\epsilon)$ vs $\ln \epsilon$ is fitted through a fourth- or fifth-order polynomial. The derivatives are calculated analytically, which give a rough overview on the dependence of the effective exponents on ϵ. (ii) Further estimates on the effective exponents were derived from a method via parabolic fits, as proposed in Ref. 12, which is used here for different values of $k=7-12$ neighboring data points.

III. RESULTS

Figure 1(a) and 1(b) show the M vs H plots for $x=0.23$ and 0.3, respectively, in the temperature range $T_C \pm 10$ K. The insets show plots of H/M vs M^2 with positive slopes indicating a second-order phase transition.[13]

Figure 2(a) and 2(b) show modified Arrott plots for $M^{1/\beta}$ vs $(H_{\text{eff}}/M)^{1/\gamma}$ constructed from the M vs H plots at different temperatures by using trial critical exponents β and γ similar to those of the three-dimensional (3D) Heisenberg magnets. For the data of $x=0.23$ crystal, this choice produces a range of nearly parallel linear isothermal curves for higher fields. This indicates that the critical properties are close to those of isotropic 3D ferromagnets. For the $x=0.30$ crystal, the modified Arrott plots display systematic nonlinearities. Other choices of trial exponents result in stronger deviations from linearity in the modified Arrott plots for both crystals. This has been checked for the values of mean field, tricritical mean field, and 3D Ising-like exponents as trial exponents. Following a standard procedure, the modified Arrott plots were extrapolated to the y-axis intercept corresponding to

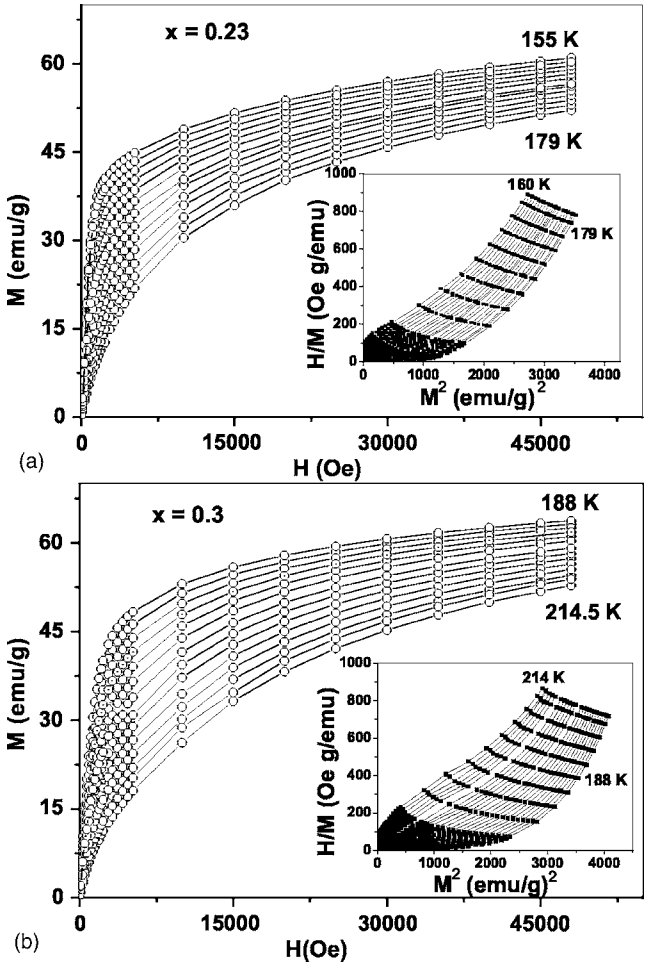

FIG. 1. Magnetization vs field of $Pr_{1-x}Pb_xMnO_3$ for (a) $x=0.23$ and (b) $x=0.30$ from 0 to 5 T around T_C. Insets show Arrott plots, H_{eff}/M vs M^2, for both compositions. The positive slopes indicate a second-order transition in both cases.

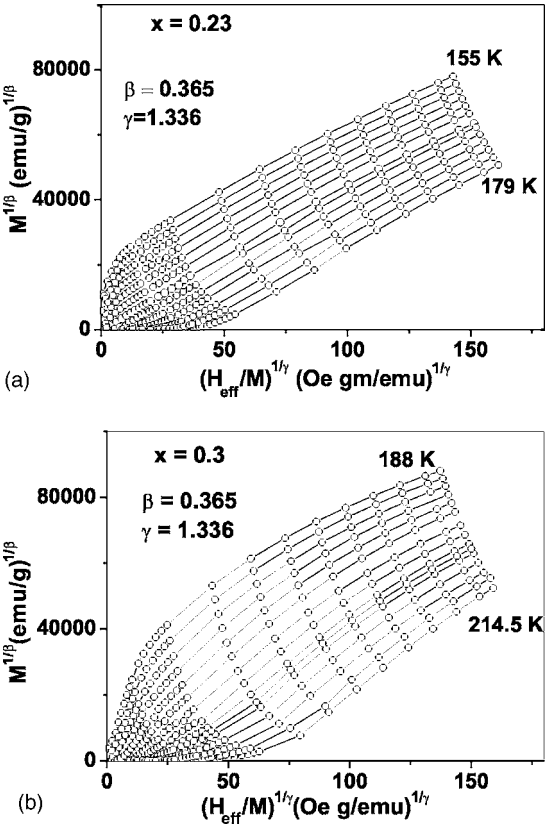

FIG. 2. Modified Arrott plots of $Pr_{1-x}Pb_xMnO_3$ for (a) $x=0.23$ and (b) $x=0.30$, where $\beta=0.365$ and $\gamma=1.336$ are the trial values corresponding to 3D Heisenberg ferromagnet.

$M_S(T,0)$. At T_C, this extrapolated line passes through the origin. The inverse initial susceptibility $\chi^{-1}(T)$ is obtained from the ratio of the y intercept and the slope above T_C. The T_C for $x=0.23$ lies between 167 and 167.5 K, while that for $x=0.30$ lies between 197.5 and 198 K. For this extrapolation, we have used the values above a field of about 0.1 T for crystal with $x=0.23$. For the crystal with $x=0.3$, roughly linear portions of the modified Arrott plot towards high fields have been used, with more low field values closer to the assumed T_C. It is clear that this approach is a compromise which averages out important physical contributions to the critical behavior. The universal scaling laws are almost obeyed with the trial values of β and γ close to those of the 3D Heisenberg universality class for $x=0.30$.

Plots of $M_S(T,0)$ vs T for both compositions are shown in Figs. 3(a) and 3(b). The values of T_C and β were obtained by fitting $M_S(T,0)$ vs T to Eq. (1). The $\chi^{-1}(T)$ vs T plots are also shown in Figs. 3(a) and 3(b). We obtain γ and T_C by fitting $\chi^{-1}(T)$ to Eq. (2). This procedure is iterated by using the derived critical exponents again in a modified Arrott plot. Thus, a check has been made that the derived critical exponents are close to the trial exponents and that the two critical temperatures T_C from the fits are the same within error estimates.

The exponents were also obtained by the Kouvel-Fisher method,[9] as shown in Figs. 4(a) and 4(b) where $M_S(T,0) \times [dM_S(T,0)/dT]^{-1}$ is plotted against T. The plots are straight lines with slope $1/\beta$, and T_C is the ratio of y intercept and slope. Similarly, in Figs. 4(a) and 4(b), we plot $\chi^{-1}(T)[d\chi^{-1}(T)/dT]^{-1}$, which shows a linear dependence. We have listed the critical exponents obtained from the modified Arrott plots as well as the Kouvel-Fisher method along with T_C in Table I. In Figs. 5(a) and 5(b), the critical isotherms M vs H for both crystals are plotted at 167 and 197.5 K for $x=0.23$ and 0.30, respectively. At the critical temperature, M and H are related by Eq. (3). The high-field region of the data is fitted by a straight line with slope $1/\delta$. The values of δ obtained for both compositions are given in Table I. The three exponents derived from our static scaling analysis are related by the Widom scaling relation

$$\delta = 1 + \gamma/\beta. \tag{6}$$

Using this scaling relation and the estimated values of β and γ, we obtain δ values which are close to the estimates for δ from the critical isotherms at T_C. Thus, the estimates of the critical exponents are consistent. In the critical region, the magnetization and applied field should obey the universal scaling behavior. In Figs. 6(a) and 6(b), we show plots of $M|\epsilon|^{-\beta}$ vs $H|\epsilon|^{-(\beta+\gamma)}$ for $x=0.23$ and 0.30, respectively. The

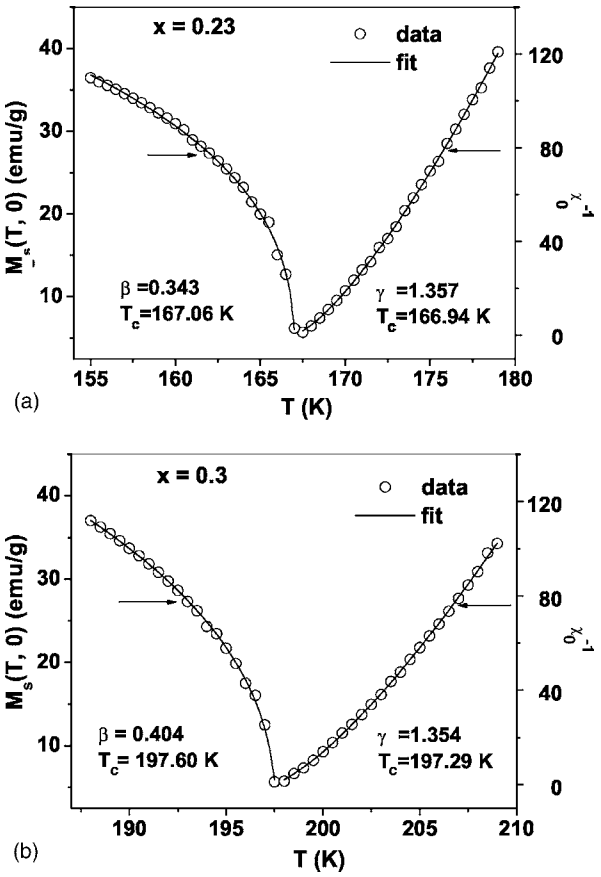

FIG. 3. Spontaneous magnetization (left) and initial susceptibility (right) vs temperature of $Pr_{1-x}Pb_xMnO_3$ for (a) $x=0.23$ and (b) $x=0.30$ to determine β and γ, respectively. [For clarity, only parts of the $M(H)$ data measured around T_C are shown in this and the next figure.]

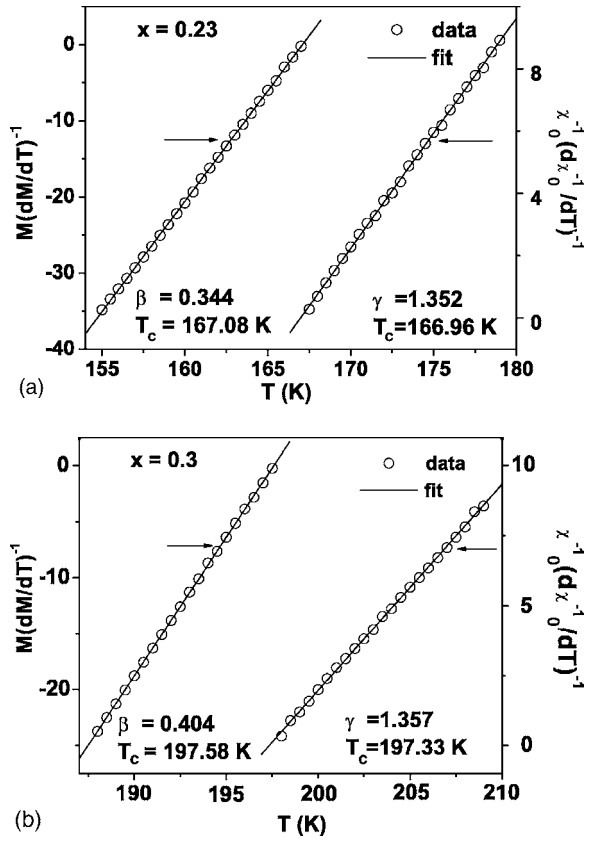

FIG. 4. Kouvel-Fisher plots of $M_S(T,0)[dM_S(T,0)/dT]^{-1}$ and $\chi^{-1}(T)[d\chi^{-1}(T)/dT]^{-1}$ vs T for determination of β and γ in $Pr_{1-x}Pb_xMnO_3$ for (a) $x=0.23$ and (b) $x=0.30$, respectively.

two curves represent temperatures below and above T_C. The insets show the same data in log-log scale.

IV. DISCUSSION

From our analysis, we see that the scaling is well obeyed for $x=0.23$. The values of critical exponents of $Pr_{0.77}Pb_{0.23}MnO_3$ are consistent with those of the 3D Heisenberg ferromagnet that has critical indices $\beta_H=0.368$, $\gamma_H=1.396$, and $\delta_H=4.80$.[14] This behavior is quite similar to other CMR manganites belonging to the universality class of 3D isotropic ferromagnets with short-range exchange couplings.[15,16] The $x=0.23$ composition is on the crossover region of a MI transition. Around T_C, there exists a small temperature range where it exhibits a metallic behavior as mentioned earlier.[5] On the other hand, the scaling is poor for the crystal with composition $x=0.3$, in particular, towards low fields. The nonlinearity in the modified Arrott plot indicates a nonconventional magnetic ordering behavior in this crystal. The T_{MI} of this composition is about 35 K above the Curie temperature T_C.[5,17] Moreover, there are systematic deviations from Curie-Weiss behavior below 250 K in this compound.[5] This may indicate the formation of ferromagnetic clusters,[17] which results in a percolation mechanism for conduction and metallic behaviors without a magnetic long-range order above T_C. The nonlinearity of modified Arrott plots in Fig. 3(b) may be attributed to the presence of ferromagnetic clusters. The clustering behavior may indicate the formation of a Griffiths phase with randomly varying local ordering temperature,[18] as proposed and described for ferromagnetic manganites in Refs. 19 and 20

Clustering in relevant models for a Heisenberg-like magnet would yield complicated crossover phenomena near criticality and nonuniversal asymptotic exponents.[10] In particular, long-range correlated quenched disorder can become relevant for Heisenberg-like magnets. Such effects are described by the Weinrib-Halperin model through correlated random-temperature defects falling off as a power law r^{-a} with distance.[21] In the case of a 3D isotropic Heisenberg-like magnet, the critical exponents in this random-temperature model continuously vary with the exponent $a<3$. From a field-theoretical calculation, values for β in the range of 0.387–0.384 and remarkably increasing values of γ in the range of 1.37–1.57 have been found.[22] On the other hand, Heisenberg-like systems may show values $\gamma>1.41$ in the presence of extended impurities with dimensionality $\varepsilon_d \geqslant 0.4$.[23] For systems with uncorrelated quenched disorder, conventional Heisenberg-like critical properties should be expected. Such conventional critical exponents have been found for the rounded PM-FM transition in $La_{0.67}Ca_{0.33}MnO_3$ with low Ga substitution on Mn sites.[24]

TABLE I. Evaluation of critical exponents of $Pr_{1-x}Pb_xMnO_3$.

	Modified Arrott plots			Kouvel-Fisher method			Critical isotherm	
Composition	β	γ	T_C (average)	β	γ	T_C (average)	δ (Expt.)	δ (Calc.) Eq. (6)
x=0.23	0.343±0.005	1.357±0.020	167.00±0.13	0.344±0.001	1.352±0.006	167.02±0.04	4.69±0.02	4.93
x=0.30	0.404±0.006	1.354±0.020	197.46±0.13	0.404±0.001	1.357±0.006	197.45±0.04	4.73±0.09	4.37

Hence, the relevant models suggest that one should expect PM-FM transition with conventional or nonuniversal critical indices in a Heisenberg-like magnet with random-temperature defects. Strong effects of such disorder would arise only if these defects display long-range correlations.

As demonstrated by the extrapolation in the modified Arrott plot for relatively large fields and the scaling plot, Fig. 6(b), we see an effective critical behavior in the crystal x =0.3 that is consistent with the properties of a Heisenberg-like magnet. In particular, the exponent γ is not significantly increased. On the other hand, in the low-field region, we see marked deviations from scaling, which are not consistent with a conventional or nonuniversal critical PM-FM behavior. Hence, the critical properties of this crystal cannot be explained by extended random-temperature effects leading to a remarkable Griffiths phase effect.

The rounding effect, as seen in the modified Arrott plot, Fig. 2(b), is pronounced close to the transition. It has been pointed out by Rivadulla *et al.*[25] that this behavior is often seen in various nominally ferromagnetic manganites. The behavior indicates a suppression of ferromagnetic order by some further coupling effects that are effective on longer ranges and may lead to frustration. In fact, the modified Arrott plots resemble those proposed from theoretical considerations for magnets with frustrated couplings of random-field or random-anisotropy type[26] as found, e.g., in experiments

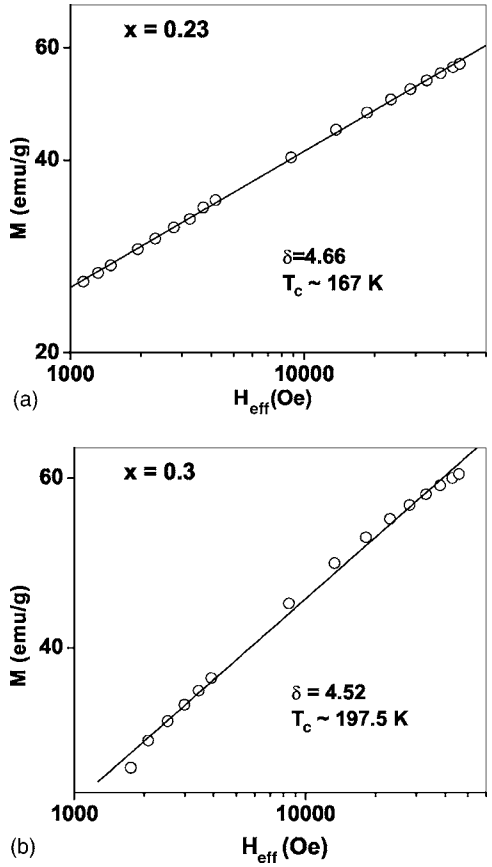

FIG. 5. Critical isotherms for $Pr_{1-x}Pb_xMnO_3$ for (a) x=0.23 and (b) x=0.30 corresponding to T_C=167 K and T_C=197.5 K, respectively.

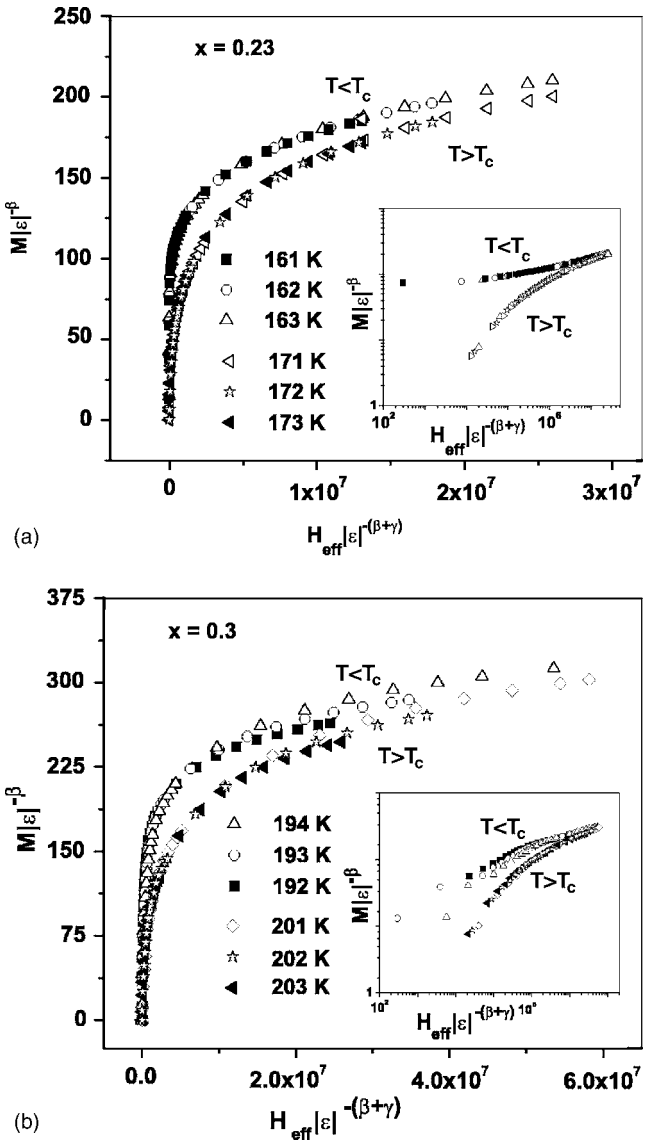

FIG. 6. Scaling plots for $Pr_{1-x}Pb_xMnO_3$ for (a) x=0.23 and (b) x=0.30, indicating two universal curves below and above T_C. The insets show the plots on a log-log scale.

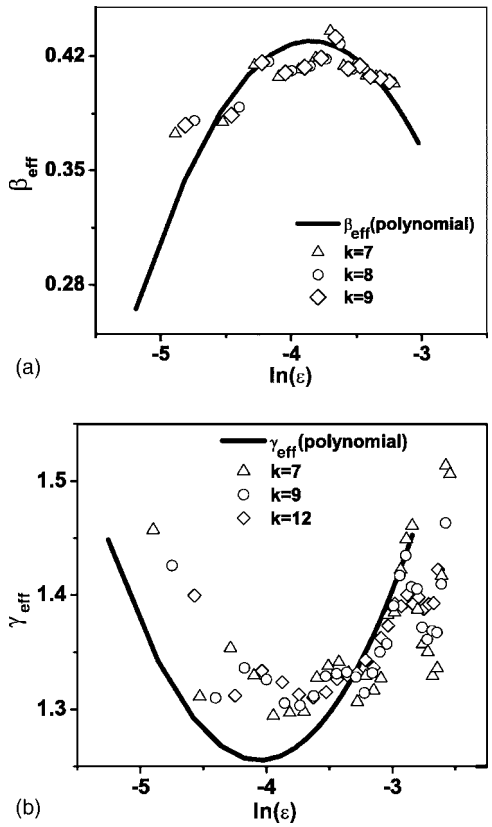

FIG. 7. Effective exponents (a) for static spontaneous magnetization β_{eff} below T_C and (b) for initial susceptibility above T_C vs reduced temperature $\ln(\epsilon)$ for $Pr_{0.70}Pb_{0.30}MnO_3$. Logarithmic derivatives, Eq. (5), are from polynomial fits (continuous thick line) and from a numeric error-improved method (Ref. 12) using k neighboring data points (symbols).

on rare-earth-based disordered magnets.[27] Based on symmetry considerations for a ferromagnetic system one expects only quenched random-anisotropy effects, which destroy long-range magnetic order in isotropic magnets.[11]

To discern the influence of such random magnetic couplings, we have plotted effective critical exponents for the crystal with composition $x=0.3$ in Figs. 7(a) and 7(b). These effective exponents have been derived by the logarithmic derivatives [Eq. (5)] for the extrapolated $M_S(T,0)$ and $\chi_0(T)$ from the modified Arrott plot. As usual, the estimates for γ_{eff} and β_{eff} are prone to large uncertainty reflected in the scatter between the results of different numerical methods used for Fig. 7. However, there is a systematic nonmonotonous shift of the exponents with decreasing ϵ. In particular, γ_{eff} increases with increasing ϵ. A maximum or increasing γ_{eff} with larger ϵ has similarly been found in a recent investigation on a frustrated metallic ferromagnet.[28] Such systematic dependencies of γ_{eff} are suggested by theoretical investigations on effective critical properties of random-anisotropy magnets.[11] From our data, we cannot determine whether a plateau is reached for the effective exponents at small ϵ. The data may also indicate a diverging γ_{eff} and vanishing β_{eff}. Such a behavior corresponds to an infinite susceptibility phase or a quasi-long-range ordered domainlike state without macroscopic spontaneous magnetization, as proposed for random-anisotropy systems.[26] A frustrated domainlike state also explains the significant deviation from the power law, Eq. (3), seen in the critical isotherm, Fig. 5(b).

Thus, the overall critical behavior seen in the static magnetization data suggests the presence of random symmetry-breaking couplings in the magnetic system of the crystal with $x=0.30$. Recent investigations on the Griffiths-like properties in paramagnetic $La_{1-x}Sr_xMnO_3$ also indicate that frustrated magnetic couplings may be present in the ferromagnetic manganites.[20] Such additional frustrating couplings explain for the $Pr_{0.70}Pb_{0.30}MnO_3$ crystal (i) the suppression of the magnetic transition temperature T_C below the MI transition temperature and the occurrence of a metal-like conductivity in a paramagnetic state, (ii) the anomalous rounding as seen in the modified Arrott plot, (iii) the markedly nonmonotonous dependence of the effective critical exponents near the magnetic ordering transition, and (iv) the rounded critical isotherm.

V. CONCLUSIONS

The static scaling analysis near the magnetic ordering on single crystals of $Pr_{1-x}Pb_xMnO_3$ for $x=0.23$ and $x=0.30$ has been performed to derive the critical exponents β, γ, and δ. These exponents were determined by extrapolating from relatively large fields. This means that we probe the system away from criticality at shorter lengths, where the exchange mechanism is dominant. The critical exponents indicate that the underlying magnetic system in both the insulating and the metallic crystal is similar to that of a conventional isotropic magnet, as is expected for the manganites. The exponents are also consistent, as the Widom scaling relation between the exponents is obeyed. For the insulating crystal with composition $x=0.23$, the data fit well with the universal scaling behavior. Thus, the magnetic properties in these crystals are those of an isotropic magnet with short-range exchange couplings. They are not subject to remarkable further effects as long-range magnetic couplings that would lead to nonuniversal or mean-field properties. However, we can discern important magnetic coupling effects, which destroy proper universal scaling for the metallic crystal with $x=0.30$. The scaling analysis as a conventional ferromagnet yields exponents, which average out the systematic drift seen in the effective exponents. Hence, there is evidence for an important crossover effect in this crystal, which intercepts the formation of the conventional magnetic long-range order by frustrated magnetic couplings.

ACKNOWLEDGMENT

One of the authors (H.L.B.) acknowledges CSIR (India) for financial support.

*Corresponding author. FAX: 91-80-360 2602. Email address: paddu@physics.iisc.ernet.in

[1] *Colossal Magnetoresistive Oxides*, edited by Y. Tokura (Gordon and Breach Science Publishers, New York, 2000).

[2] *Colossal Magnetoresistance, Charge Ordering and Relative Properties of Magnetic Oxides*, edited by C. N. R. Rao and B. Raveau (World Scientific, Singapore, 1998).

[3] W. Archibald, J. S. Zhou, and J. B. Goodenough, Phys. Rev. B **53**, 14445 (1996).

[4] Y. Motome and N. Furukawa, J. Phys. Soc. Jpn. **70**, 1487 (2001).

[5] B. Padmanabhan, Suja Elizabeth, H. L. Bhat, Sahana Rössler, K. Dörr, and K. H. Müller, J. Magn. Magn. Mater. **307**, 288 (2006).

[6] J. Hemberger, A. Krimmel, T. Kurz, H.-A. Krug von Nidda, V. Yu. Ivanov, A. A. Mukhin, A. M. Balbashov, and A. Loidl, Phys. Rev. B **66**, 094410 (2002).

[7] G. V. Pai, S. R. Hassan, H. R. Krishnamurthy, and T. V. Ramakrishnan, Europhys. Lett. **64**, 696 (2003).

[8] A. H. Morrish, B. J. Evans, J. A. Eaton, and L. K. Leung, Can. J. Phys. **47**, 2691 (1969).

[9] J. S. Kouvel and M. E. Fisher, Phys. Rev. **136**, A1626 (1964).

[10] M. Dudka, R. Folk, Yu. Holovatch, and D. Ivaneiko, J. Magn. Magn. Mater. **256**, 243 (2003).

[11] M. Dudka, R. Folk, and Yu. Holovatch, J. Magn. Magn. Mater. **294**, 305 (2005).

[12] A. Möbius, C. Frenzel, R. Thielsch, R. Rosenbaum, C. J. Adkins, M. Schreiber, H. D. Bauer, R. Grötzschel, V. Hoffmann, T. Krieg, N. Matz, H. Vinzelberg, and M. Witcomb, Phys. Rev. B **60**, 14209 (1999).

[13] J. Mira, J. Rivas, F. Rivadulla, C. Vazquez-Vazquez, and M. A. Lopez-Quintela, Phys. Rev. B **60**, 2998 (1999).

[14] M. Campostrini, M. Hasenbusch, A. Pelissetto, P. Rossi, and E. Vicari, Phys. Rev. B **65**, 144520 (2002).

[15] M. Sahana, U. K. Rössler, N. Ghosh, S. Elizabeth, H. L. Bhat, K. Dörr, D. Eckert, M. Wolf, and K. H. Müller, Phys. Rev. B **68**, 144408 (2003).

[16] Nilotpal Ghosh, Sahana Rössler, U. K. Rössler, K. Nenkov, Suja Elizabeth, H. L. Bhat, K. Dörr, and K.-H. Müller, J. Phys.: Condens. Matter **18**, 557 (2006).

[17] Run-Wei Li, Xin Zhou, Bao-Gen Shen, and Burkhard Hillebrands, Phys. Rev. B **71**, 092407 (2005).

[18] R. B. Griffiths, Phys. Rev. Lett. **23**, 17 (1969).

[19] M. B. Salamon, P. Lin, and S. H. Chun, Phys. Rev. Lett. **88**, 197203 (2002); M. B. Salamon and S. H. Chun, Phys. Rev. B **68**, 014411 (2003).

[20] J. Deisenhofer, D. Braak, H.-A. Krug von Nidda, J. Hemberger, R. M. Eremina, V. A. Ivanshin, A. M. Balbashov, G. Jug, A. Loidl, T. Kimura, and Y. Tokura, Phys. Rev. Lett. **95**, 257202 (2005).

[21] A. Weinrib and B. I. Halperin, Phys. Rev. B **27**, 413 (1983).

[22] V. V. Prudnikov, P. V. Prudnikov, and A. A. Fedorenko, J. Phys. A **32**, 8587 (1999).

[23] V. Blavats'ka, C. von Ferber, and Yu. Holovatch, Phys. Rev. B **67**, 094404 (2003).

[24] S. Röszler, U. K. Röszler, K. Nenkov, D. Eckert, S. M. Yusuf, K. Dörr, and K.-H. Müller, Phys. Rev. B **70**, 104417 (2004).

[25] F. Rivadulla, J. Rivas, and J. B. Goodenough, Phys. Rev. B **70**, 172410 (2004).

[26] A. Aharony and E. Pytte, Phys. Rev. Lett. **45**, 1583 (1980).

[27] P. M. Gehring, M. B. Salamon, A. del Moral, and J. I. Arnaudas, Phys. Rev. B **41**, 9134 (1990).

[28] A. Perumal, V. Srinivas, V. V. Rao, and R. A. Dunlap, Phys. Rev. Lett. **91**, 137202 (2003).